An EPR Spectroscopic Study of Chromium(V) Oxalato Complexes in Aqueous Solutions. Mechanism of the Chromium(VI) Oxidation of Oxalic Acid

Rodney P. Farrell,[†] Peter A. Lay,*[,†] Aviva Levina,[†] Ian A. Maxwell,[†] Richard Bramley,[‡] Steven Brumby,[‡] and Ji-Ying Ji[‡]

School of Chemistry, University of Sydney, 2006 Sydney, Australia, and Research School of Chemistry, Australian National University, 0200 Canberra, Australia

Received August 21, 1997

Chromium(V) oxalato complexes have been of considerable interest as intermediates in the Cr(VI) oxidation of oxalic acid, which is used as a prototype in mechanistic studies of Cr(VI) oxidations of organic substrates. These complexes have been characterized by X-band EPR spectroscopy from the reactions of Cr(VI) (CrO_3) or Cr(V) ($Na[Cr^VO(ehba)_2]$; ehba = 2-ethyl-2-hydroxybutanoate(2−)) with oxalic acid (oxH_2) in acidic aqueous solutions (pH = 0−1.5; I = 1 M ($HClO_4/NaClO_4$); 21 °C). Structures and formation mechanisms of these complexes have been deduced from the dependences of the relative intensities of the corresponding EPR signals (obtained by digital simulations of the EPR spectra) on the reaction conditions. A range of Cr(V) complexes, including five-coordinate species, $[Cr^V(O)_2(OH_2)(ehba)]^-$, $[Cr^VO(ehba)(ox)]^-$, and $[Cr^VO(ox)_2]^-$, and six-coordinate species, $[Cr^VO(OH_2)(ox)_2]^-$, $[Cr^VO(OH)(ox)_2]^{2-}$, $[Cr^VO(oxH)(ox)_2]^{2-}$, and possibly $[Cr^V(O)_2(OH_2)_2(ox)]^-$, as well as mixed-valence Cr(III)−Cr(V) dimers and trimers and Cr(VI)−Cr(V) species, such as $[Cr^VCr^{VI}(O)_5(OH_2)(ox)_2]^{3-}$, have been characterized. Apart from the first detailed characterization of these species, this is the first spectral evidence for the existence of mixed-valence Cr(V)−Cr(VI) complexes. On the basis of quantitative analysis of EPR spectra for the Cr(VI)−oxH_2 system, Cr(VI) has been shown to exist mainly in the form of the monooxalato complex, $[Cr^{VI}(O)_2(OH)(ox)]^-$ in the presence of excess oxH_2. The data on the structures and reactivities of Cr(V) and Cr(VI) oxalato complexes have been used to propose a new mechanism for the Cr(VI) oxidation of oxH_2 in acidic aqueous solutions.

Introduction

Chromium(V) chemistry has received a considerable degree of recent attention for two main reasons.[1−4] First, Cr(VI) is used widely as a selective oxidant in fine organic chemicals syntheses, and Cr(V) intermediates are commonly formed in the reactions of Cr(VI) with organic substances.[1,2] Therefore, elucidations of the structures, formation, and decomposition mechanisms of Cr(V) intermediates are required for the optimization of reactions using Cr(VI) as an oxidant, as well as for creation of catalytic processes, using only small amounts of environmentally hazardous[4] Cr compounds in combination with environmentally safe oxidants (O_2 or H_2O_2).[5] Second, Cr(V) complexes with biomolecules have been implicated as important intermediates in Cr(VI)-induced genotoxicities.[2,4,6] Therefore, a knowledge of Cr(V) chemistry is required to elucidate the mechanisms of such genotoxicities and to suggest possible preventive measures for them. As most of the known Cr(V) compounds are EPR-active at room temperature due to their d^1 electronic configuration, EPR spectroscopy has become the most powerful technique for studies of Cr(V) chemistry.[3]

The reaction of Cr(VI) with oxalic acid (oxH_2) in acidic aqueous solutions has been a subject of detailed kinetic investigations[7] as a convenient model for elucidation of the general rules of Cr(VI) redox chemistry. Although the detection of Cr(V) species in this reaction by EPR spectroscopy was reported more than 20 years ago,[8] the structures of these species remained unclear. As a part of the current research program targeted toward a better understanding of the structures and reactivities of Cr(V) complexes in aqueous solutions,[2,3,6] we have undertaken an EPR-spectroscopic investigation of Cr(V) oxalato complexes formed in the Cr(VI) + oxH_2 and Cr(V) + oxH_2 reactions. Preliminary results of this work have been published.[3,9−11] However, the quantitative interpretation of the previous results[9−11] was complicated due to the following

[†] University of Sydney.
[‡] Australian National University.

(1) Mitewa, M.; Bontchev, R. *Coord. Chem. Rev.* **1985**, *61*, 214−272 and references therein.
(2) Farrell, R. P.; Lay, P. A. *Comments Inorg. Chem.* **1992**, *13*, 133−175 and references therein.
(3) Barr-David, G.; Charara, M.; Codd, R.; Farrell, R. P.; Irwin, J. A.; Lay, P. A.; Bramley, R.; Brumby, S.; Ji, J.-Y.; Hanson, G. R. *J. Chem. Soc., Faraday Trans.* **1995**, *91*, 1207−1216 and references therein.
(4) (a) Kortenkamp, A.; Casadevall, M.; Da Cruz Fresco, P.; Shayer, R. O. J. *NATO ASI Ser., Ser. 2* **1997**, *26*, 15−34. (b) Stearns, D. M.; Wetterhahn, K. E. *NATO ASI Ser., Ser. 2* **1997**, *26*, 55−72 and references therein.
(5) Muzart, J. *Chem. Rev.* **1992**, *92*, 113−140.
(6) (a) Farrell, R. P.; Judd, R. J.; Lay, P. A.; Dixon, N. E.; Baker, R. S. U.; Bonin, A. M. *Chem. Res. Toxicol.* **1989**, *2*, 227−229. (b) Dillon, C. T.; Lay, P. A.; Bonin, A. M.; Dixon, N. E.; Collins, T. J.; Kostka, K. L. *Carcinogenesis* **1993**, *14*, 1875- 1880.
(7) Hasan, F.; Roček, J. *J. Am. Chem. Soc.* **1972**, *94*, 9073−9081 and references therein.
(8) Srinivasan, V.; Roček, J. *J. Am. Chem. Soc.* **1974**, *96*, 127−133.
(9) Farrell, R. P.; Judd, R. J.; Lay, P. A.; Bramley, R.; Ji, J.-Y. *Inorg. Chem.* **1989**, *28*, 3401−3403.
(10) Bramley, R.; Farrell, R. P.; Ji, J.-Y.; Lay, P. A. *Aust. J. Chem.* **1990**, *43*, 263−269.
(11) Farrell, R. P. Ph.D. Thesis, University of Sydney, 1993.

S0020-1669(97)01070-7 CCC: $15.00
Published on Web 06/05/1998

reasons: (i) the range in the reaction conditions and the number of experiments were small; (ii) the ionic strength was not kept constant; and (iii) in most cases, the reactions were carried out in 50% aqueous acetic acid, which led to the formation of a range of mixed acetato−oxalato Cr(V) complexes. The current work presents a detailed quantitative study of Cr(V) oxalato complexes formed in aqueous perchlorate solutions under a wide range of reaction conditions.

Experimental Section

Caution! *Chromium(VI) compounds are human carcinogens,*[12] *and Cr(V) complexes are mutagenic and potentially carcinogenic.*[6] *Contact with skin and inhalation must be avoided.*

Reagents. The following commercial reagents of analytical or higher purity grade were used as received: 2-ethyl-2-hydroxybutanoic acid ($ehbaH_2$) and tetrahydrothiophene 1,1-dioxide (sulfolane) from Aldrich; $H_2C_2O_4{\cdot}2H_2O$, $NaClO_4{\cdot}H_2O$, $HClO_4$, and NaOH from Fluka; CrO_3, $Na_2Cr_2O_7{\cdot}2H_2O$, $Na_2CrO_4{\cdot}4H_2O$, and $Cr(NO_3)_3{\cdot}9H_2O$ from Merck. Water was purified by the Milli-Q technique. Sodium bis(2-ethyl-2-hydroxybutanoato(2−))oxochromate(V) monohydrate was synthesized by the method of Krumpolc and Roček[13] and its purity was confirmed by UV−visible and EPR spectroscopies.

Methods and Equipment. X-band EPR spectra of Cr(V) complexes were recorded at 21 ± 1 °C, using a flat quartz cell with a Bruker ESP 300 spectrometer, equipped with a HP 5352B frequency counter and a Bruker ER 035M gaussmeter. Typical parameters for acquisition of EPR spectra were as follows: center field, 3500 G; sweep width, 100 G; resolution, 1024 points; microwave frequency, ∼9.66 GHz; microwave power, 10 mW; modulation frequency, 100 kHz; modulation amplitude, 0.97 G; time constant, 1.28 ms; sweep time, 5.24 s; number of scans, 20; and receiver gain, (1−50) × 10^4. Unless specifically noted, EPR spectra were acquired at 3−4 min after preparation of the reaction solutions. In all experiments, the ionic strength was kept constant (I = 1.0 M; $HClO_4$ + $NaClO_4$). For the experiments with the variation of $[H_2O]$, sulfolane was chosen as a highly polar, chemically inert, and, most importantly, weakly coordinating cosolvent.[14] Therefore, it was anticipated that sulfolane molecules will not replace the ligands in Cr(V) complexes. The following ranges of reaction conditions were used: (i) for the Cr(V)−$ehbaH_2$−oxH_2 system, $[Cr(V)]_0$ = 0.010−0.10 mM, $[ehbaH_2]_0$ = 1.0−5.0 mM, $[oxH_2]_0$ = 25−150 mM, $[HClO_4]$ = 0−1.0 M, $[H_2O]$ = 54 M (without additions of sulfolane); and (ii) for the Cr(VI) + oxH_2 system, $[Cr(VI)]_0$ = 2.5−20 mM; $[oxH_2]_0$ = 10−100 mM; $[HClO_4]$ = 0−1.0 M; $[H_2O]$ = 27−54 M. Typically, concentrated solutions of Cr(V) or Cr(VI) were added to the solutions containing the required concentrations of oxH_2, $ehbaH_2$, and $HClO_4$. For the experiments with added Cr(III), solutions containing $Cr(NO_3)_3$, oxH_2, and $HClO_4$ were preequilibrated (by heating at ∼100 °C for 30 min and then cooling to room temperature) before the addition of Cr(VI). An Activon 210 ionometer equipped with an AEP 321 glass-calomel electrode was used for pH measurements.

Processing of EPR Spectra. Initially, digital simulations of EPR spectra were performed by Spectrum Analysis Package software;[15] final simulation results were obtained with the use of WinSim EPR simulation software.[16] In both simulation methods, Lorentzian line shapes and simplex optimization procedures were used for calculation of the positions, widths, and relative areas of EPR signals.[17] Maximal deviations between the experimental and simulated spectra were 20−25% (typical examples are shown in Figures S1 and S2, Supporting Information). Therefore, the minor signals due to hyperfine coupling of the ^{53}Cr isotope (∼9 atom% Cr, resulting in four signals of ∼2.3% of the major signal) were neglected in the simulations. For each spectrum, three to five independent simulations were performed with the use of different sets of initial parameters. The differences in the values of line widths and relative areas, obtained from the parallel simulations, were up to 15% for major and well-resolved signals, and up to 30% for minor and overlapped signals. Averaged results of at least three parallel simulations were used for statistical analysis (performed with the use of Origin and Excel software)[18] of the dependences between the parameters of EPR spectra and the reaction conditions. The parameters of the reaction medium, used for the statistical analysis, were determined as follows: (i) correlations between pH and $[H^+]$ values at I = 1.0 M were established by pH-metric titrations of $HClO_4$ solutions by NaOH;[19] (ii) pK_a values at I = 1.0 M for $ehbaH_2$ (3.30 ± 0.05) and oxH_2 (1.25 ± 0.05, 4.25 ± 0.05) were determined by potentiometric titrations; and (iii) concentrations of undissociated oxH_2 were determined as

$$[oxH_2] = [oxH_2]_0[H^+]/([H^+] + K_a) \quad (1)$$

for the Cr(V)−$ehbaH_2$−oxH_2 system and

$$[oxH_2] = ([oxH_2]_0 - X[Cr(VI)]_0)[H^+]/([H^+] + K_a) \quad (2)$$

for the Cr(VI)−oxH_2 system, where $K_a = 5.62 \times 10^{-2}$ is the first deprotonation constant for oxH_2 and X = 0.13−1.0 is the coefficient for the extent of the complexation of oxH_2 with Cr(VI) (see Results).

For $ehbaH_2$, only the undissociated form was assumed to exist under the reaction conditions, on the basis of its pK_a value (see above).

Results

The Cr(V)−ehbaH$_2$−oxH$_2$ System. Addition of $Na[Cr^VO(ehba)_2]$ to acidic solutions of oxH_2 results in EPR spectra consisting of three major signals (**1**, **3**, **5**) and three minor ones (**2**, **4**, **6**) (Figure 1, Table 1). The EPR signals disappear after ∼20 min (21 °C) due to the reduction of Cr(V) to Cr(III) by oxH_2. The results of quantifying the speciation by digital simulations of 33 EPR spectra are summarized in Table S1, Supporting Information. The following dependences among the relative intensities of the signals **1**−**6** and the reaction conditions have been established. An increase of $[ehbaH_2]_0$ (at constant $[oxH_2]_0$ and $[H^+]$) led to the growth of signal **1** at the expense of signals **2**, **3**, and **5** (Figure 1a,b). However, the relative areas of the signals were determined by the ratio $[ehbaH_2]/[oxH_2]$ rather than by individual concentrations of $ehbaH_2$ and oxH_2 (Table S1). A decrease in $[H^+]$ also led to a relative increase of signal **1** (Figure 1a,c). The weak signal **4** appeared at $[H^+] \leq 0.25$ M (Figure 1c). Variations in the $[Cr(V)]_0$ and in the reaction time did not lead to significant changes in relative areas of the separate signals (Table S1). It was noted that the ratio of the areas of signals **3** and **5** was practically independent of the reaction conditions. Signal **4**, observed in the Cr(V)−$ehbaH_2$−oxH_2 system, had a very small relative intensity and could not be quantified accurately. The relative areas of the broad signal **6** were 9−12% in all experiments. No obvious dependences between the intensity of this signal and the reaction conditions were revealed (Table S1). Statistical analyses of the abovementioned dependences led to eqs 3−5:

(12) International Agency for Research on Cancer (IARC). *IARC Monogr. Eval. Carcinog. Risk Chem. Hum. Suppl.* **1987**, *7*, 165−168.
(13) Krumpolc, M.; Roček, J. *J. Am. Chem. Soc.* **1979**, *101*, 3206−3209.
(14) Arnett, E. M.; Douty, C. F. *J. Am. Chem. Soc.* **1964**, *86*, 409−412.
(15) Beckwith, A. L.; Brumby, S. *J. Magn. Reson.* **1987**, *73*, 252−267.
(16) Duling, D. R. *J. Magn. Reson.* **1994**, *B104*, 105−110. The software is available from the Internet (http://alfred.niehs.nih.gov/LMB/pest/).
(17) EPR experiments with varied microwave power did not reveal any selective saturation of separate EPR signals.[11] Therefore, the relative areas of EPR signals, estimated by digital simulations, are directly proportional to the concentrations of corresponding EPR-active species.
(18) (a) *Origin. Technical Graphics and Data Analysis for Windows*, Version 4.1; Microcal Software Inc.: Northampton, MA, 1996. (b) *Excel for Windows*, Version 4.0; Microsoft Corporation: Redmond, 1992.
(19) Irving, H.; Miles, M. G.; Pettit, L. D. *Anal. Chim. Acta* **1967**, *38*, 475−488.

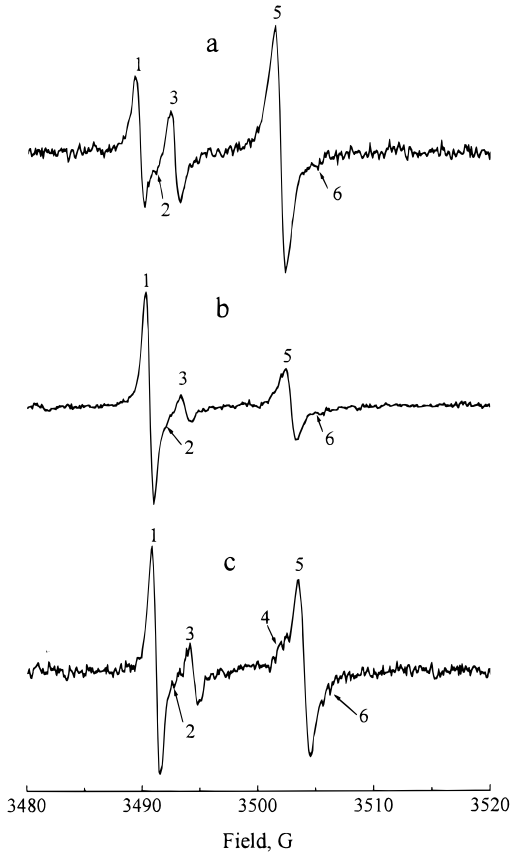

Figure 1. Influence of [ehbaH_2] and [$HClO_4$] on the EPR spectra of the Cr(V)−ehbaH_2−oxH_2 system; [Cr(V)]$_0$ = 0.050 mM, [oxH_2]$_0$ = 50 mM: (a) [ehbaH_2]$_0$ = 2.0 mM, [$HClO_4$] = 1.0 M; (b) [ehbaH_2]$_0$ = 5.0 mM, [$HClO_4$] = 1.0 M; and (c) [ehbaH_2]$_0$ = 2.0 mM; [$HClO_4$] = 0.10 mM.

Table 1. EPR-Spectroscopic Characteristics of the Cr(V) Complexes (Figures 1−4, Schemes 1 and 2)

species	g_{iso}[a]	A_{iso},[b] 10^{-4} cm^{-4}	species	g_{iso}[a]	A_{iso},[b] 10^{-4} cm^{-4}
1	1.9781	17.1	**5**	1.9710	20.1
2	1.9774	*c*	**6**	1.9703[d]	*c*
3	1.9763	16.8	**7**	1.9678[e]	19.7
4	1.9717	*c*			

[a] Error ±0.0001. [b] Hyperfine coupling of ^{53}Cr, error ±0.1. [c] Cannot be determined because of high noise level or overlap of the signals. [d] Error ±0.0003. [e] At [H_2O] = 54 M.

$$[\mathbf{1}]/[\mathbf{3}] = (0.22 \pm 0.05)[\text{ehba}H_2]/[\text{ox}H_2]^2 + ((5 \pm 1) \times 10^2)[\text{ehba}H_2]^2/[\text{ox}H_2]^2 \quad (3)$$

$$[\mathbf{2}]/[\mathbf{3}] = (9 \pm 2)[\text{ehba}H_2]/[\text{ox}H_2] \quad (4)$$

$$[\mathbf{5}]/[\mathbf{3}] = 3.4 \pm 0.8 \quad (5)$$

where [oxH_2] was estimated from eq 1.

Relative deviations between the values of [**1**]/[**3**], [**2**]/[**3**], or [**5**]/[**3**], obtained from the digital simulations of EPR spectra, and the corresponding values estimated from eqs 3−5 did not exceed 30% (typically 5−15%, see Figure S3 and Table S1 in the Supporting Information). Thus, eqs 3−5 describe the dependences between relative intensities of separate EPR signals and the reaction conditions within the precision of the simulation procedure (see Experimental Section).

The Cr(VI)−oxH_2 System. As reported previously,[8−10] the reactions of Cr(VI) with oxH_2 in acidic aqueous solutions led to the formation of Cr(V) intermediates, which could be easily observed by EPR spectroscopy. Within a 10% experimental error, identical EPR spectra were obtained using CrO_3, $Na_2Cr_2O_7$, or Na_2CrO_4 as the sources of Cr(VI) (provided that [H^+] and [oxH_2] were constant). However, CrO_3 was used as a source of Cr(VI) in most experiments. The intensities of the Cr(V) EPR signals decreased with decreasing acidity (pH = 0−1.5) such that no EPR signals were observed at pH > 1.6. The intensities of the Cr(V) EPR signals increased during the first 10−15 min of the Cr(VI) + oxH_2 reaction, and then decayed over 3−4 h (21 °C). The results of quantifying the speciation by digital simulations for 85 EPR spectra are summarized in Table S2, Supporting Information. Typical EPR spectra (Figures 2−4) consisted of signals **3**−**6**, analogous to those observed in the Cr(V)−ehbaH_2−oxH_2 system (the analogy was established on the basis of identical g_{iso} values, Table 1), and a new signal **7**.[20,21] As the reaction proceeded, a substantial broadening of the EPR signals occurred, and the relative intensities of **4** and **7** decreased and that of **6** increased (Figure 2a,b). Addition of Cr(III) caused similar effects, except for the unchanged intensity of signal **7** (Figure 2c). An increase in the [oxH_2]$_0$ led to an increase in the relative signal intensity of

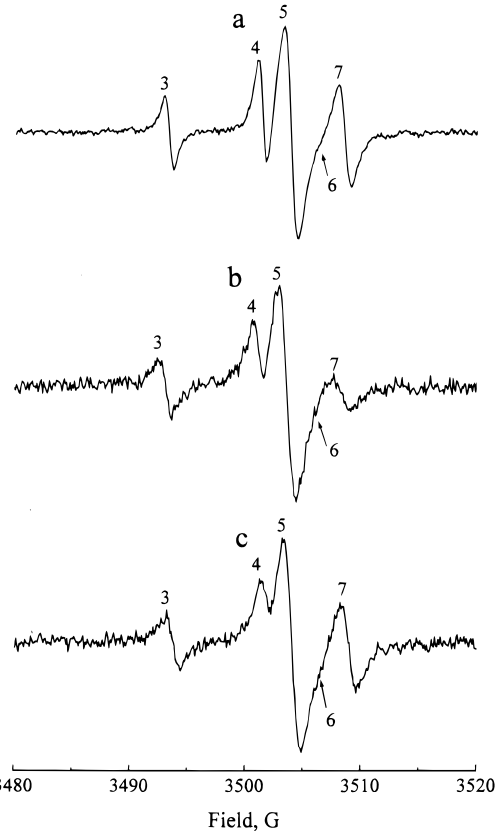

Figure 2. Influence of the reaction time and [Cr(III)] on the EPR spectra of the Cr(VI)−oxH_2 system; [Cr(VI)]$_0$ = 5.0 mM, [oxH_2]$_0$ = 50 mM, [H_2O] = 54 M, pH = 1.3: (a) reaction time 3 min; (b) reaction time 129 min; and (c) reaction time 3 min, in the presence of 5.0 mM Cr(III).

(20) In the Cr(VI)−oxH_2 system, the EPR signals due to **6** were larger than the corresponding signals in the Cr(V)−ehbaH_2−oxH_2 system and strongly overlapped with the signals due to **5**. Therefore, attempts to simulate the signals due to **5** and **6** separately were unsuccessful for the Cr(VI)−oxH_2 system.

(21) The preliminary results of Q-band (∼34 GHz) EPR spectroscopy, as well as the low-temperature (100 K) EPR experiments, did not give evidence for the formation of any other EPR-active species in the Cr(VI)−oxH_2 system.[11]

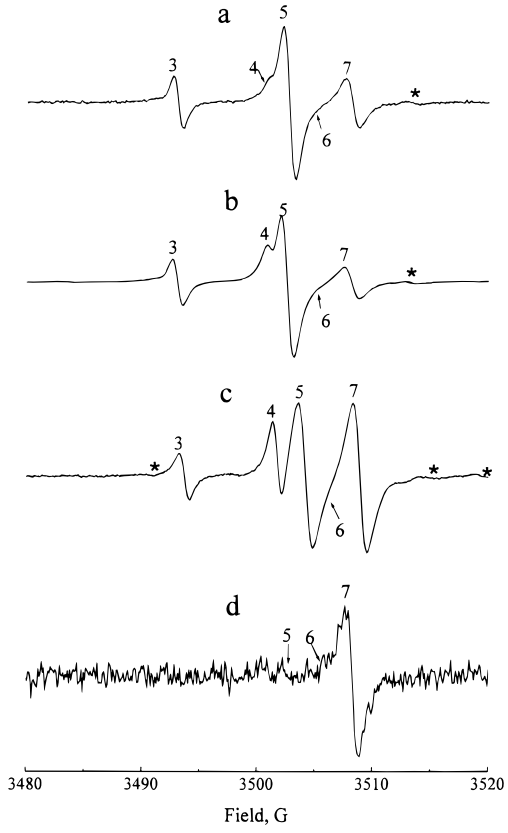

Figure 3. Influence of pH and $[oxH_2]_0$ on the EPR spectra of the Cr(VI)−oxH_2 system; $[Cr(VI)]_0 = 20$ mM, $[H_2O] = 54$ M: (a) $[oxH_2]_0 = 20$ mM, pH = 0.75; (b) $[oxH_2]_0 = 60$ mM, pH = 0.75; (c) $[oxH_2]_0 = 60$ mM, pH = 1.3; and (d) $[oxH_2]_0 = 20$ mM, pH = 1.3. The minor signals designated by asterisks are due to the hyperfine coupling of ^{53}Cr.

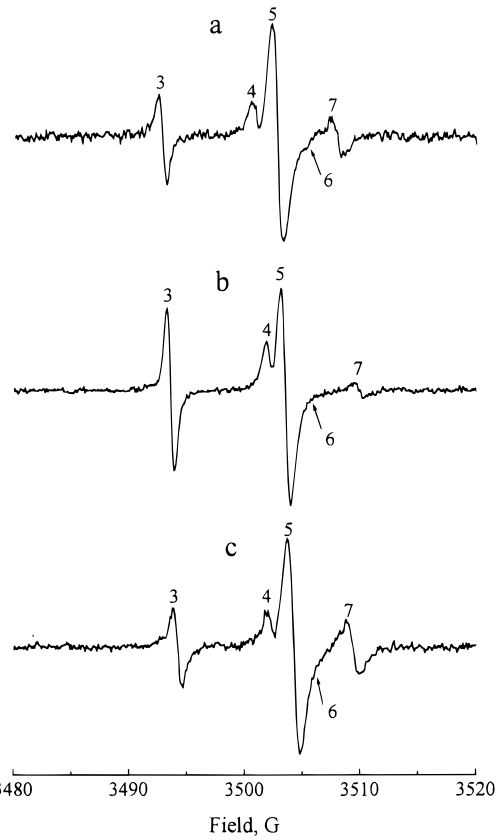

Figure 4. Influence of $[H_2O]$ and $[Cr(VI)]_0$ on the EPR spectra of the Cr(VI)−oxH_2 system; $[oxH_2]_0 = 25$ mM, $[HClO_4] = 0.10$ M: (a) $[Cr(VI)]_0 = 2.5$ mM, $[H_2O] = 54$ M (without sulfolane); (b) $[Cr(VI)]_0 = 2.5$ mM, $[H_2O] = 27$ M (4.3 M sulfolane); and (c) $[Cr(VI)]_0 = 5.0$ mM; without sulfolane.

4 and a decrease in that of **7** (Figure 3a,b). A decrease in acidity led to a substantial increase in the signal intensities of **4**, **6**, and **7** (Figure 3b,c). At low $[H^+]$ and $[oxH_2]$, and high $[Cr(VI)]_0$, **7** became the main EPR signal (Figure 3d). Changes in the time of sampling after commencement of the reaction, the $[oxH_2]_0$, and the $[H^+]$ did not affect the ratio of signal intensities for **3** and **5** (Figures 2 and 3). However, an increase in the relative intensity of **3** with respect to **5** was observed upon a decrease in the $[H_2O]$ (Figure 4a,b). A decrease in the $[H_2O]$ also led to diminished intensities for signals **6** and **7** and to a shift of signal **7** to lower g_{iso} values (Figure 4a,b). The effects of increasing the $[Cr(VI)]_0$ were a significant increase in the relative signal intensity of **7** and a small decrease in that of **4** (Figure 4a,c). The above-mentioned influences of the reaction conditions on EPR spectra observed for the Cr(VI)−oxH_2 system are quantitatively described by eqs 6−8:

$$[\mathbf{4}]/[\mathbf{3}] = (1.8 \pm 0.4)[oxH_2]/[H^+] + ((6 \pm 1) \times 10^{-4})[H_2O]/[H^+] \quad (6)$$

$$[\mathbf{5} + \mathbf{6}]/[\mathbf{3}] = ((7 \pm 1) \times 10^{-2})[H_2O] + ((7 \pm 2) \times 10^{-5})[H_2O]/([H^+][oxH_2]) \quad (7)$$

$$[\mathbf{7}]/[\mathbf{3}] = ((1.5 \pm 0.4) \times 10^{-4})X[Cr(VI)]_0[H_2O]^2/([H^+][oxH_2]) \quad (8)$$

where $[oxH_2]$ was estimated from eq 2.

Relative deviations between the values of [**4**]/[**3**], [**5** + **6**]/[**3**], or [**7**]/[**3**], obtained from digital simulations of EPR spectra, and the corresponding values estimated from eqs 6−8 were 5−25%, except for the experiments with prolonged reaction times, or in the presence of added Cr(III) (Figure S4 and Table S2 in Supporting Information). Thus, eqs 6−8 describe the quantitative determination of the concentrations of the species giving rise to the signals in the EPR spectra, within the precision of the digital simulation procedure (see Experimental Section). In most experiments, where $[oxH_2]_0 \geq 5[Cr(VI)]_0$, the *X* values in eqs 2 and 8 were equal to 1.0, suggesting that, under these conditions, Cr(VI) exists mainly as the monooxalato complex. However, for the experiments with $[Cr(VI)]_0 = 20$ mM and $[oxH_2]_0 = 10-100$ mM, *X* values were within the range 0.13−0.95, which points to the presence of several forms of Cr(VI). The *X* values for all experiments are enumerated in Table S2.

Discussion

Solution Structures of Cr(V) Oxalato Complexes. The Cr(V)−ehbaH_2−oxH_2 and Cr(VI)−oxH_2 systems are among the best models for EPR-spectroscopic studies of Cr(V) intermediates formed during the reductions of Cr(VI) and Cr(V) by organic substrates. This is due to the formation of a number of well-resolved, singlet (due to the absence of ^1H superhyperfine coupling) EPR signals. Electrochemical studies[9−11,22] have shown that ligand exchange reactions of Cr(V) oxalato complexes occur on the millisecond to second time scale, which is slow compared to the time scale of EPR spectroscopy (microseconds), but fast in comparison with the rates of the Cr(V) +

(22) Eckert, J. M.; Judd, R. J.; Lay, P. A. *Inorg. Chem.* **1987**, *26*, 2191−2192.

Scheme 1. Equilibria among Different Cr(V) Complexes in the Cr(V)−ehbaH_2−oxH_2 and Cr(VI)−oxH_2 Systems

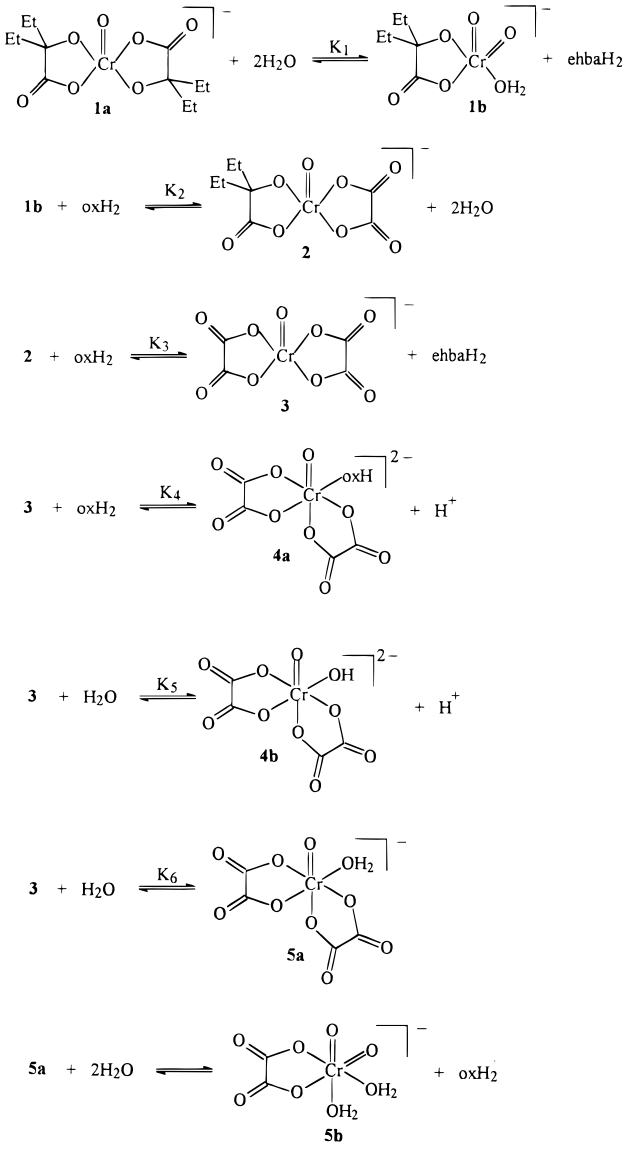

oxH_2 and Cr(VI) + oxH_2 redox reactions. Thus, the observed intensities in the EPR spectra (Figures 1−4) can be used to quantify the relative equilibrium concentrations of the Cr(V) oxalato complexes. The structures assigned to the EPR-active complexes giving rise to signals **1**−**7**, and the proposed mechanisms of ligand exchange reactions leading to these species, are presented in Schemes 1 and 2 (designations of the species correspond to those of the EPR signals in Figures 1−4 and Table 1). The corresponding equilibrium constants are enumerated in Table 2. An example of the estimated pH dependences for the speciation of the Cr(V) oxalato complexes is given in Figure S5, Supporting Information. The criteria for assigning structures rely on a number of independent observations. These include (i) the [ehbaH_2] and [oxH_2] dependences of the EPR signals resulting from the ligand exchange reactions of crystallographically characterized[23] Na[$Cr^{V}O$(ehba)$_2$] (eqs 3−5, Figure 1); (ii) the [H^+], [oxH_2], [H_2O], [Cr(VI)], and [Cr(III)] dependences of the EPR signal intensities for the Cr(V) oxalato complexes formed during the Cr(VI) + oxH_2 reaction

Table 2. Equilibrium Constants for the Ligand Exchange in Cr(V) Complexes (Schemes 1 and 2)[a]

constant	value	constant	value
K_1,[b] M	$(4 \pm 1) \times 10^{-4}$	K_5	$(6 \pm 1) \times 10^{-4}$
K_2,[b] M^{-1}	42 ± 9	K_6, M^{-1}	$(6.3 \pm 0.5) \times 10^{-2}$ [c]
K_3	$(1.1 \pm 0.2) \times 10^{-1}$		$(7 \pm 1) \times 10^{-2}$ [d]
K_4	1.8 ± 0.4	K_7	$(2.4 \pm 0.4) \times 10^{-6}$

[a] All of the constants have been estimated at 21 ± 1 °C, I = 1.0 M. [b] [H_2O] = 54 M. [c] The Cr(V)−ehbaH_2−oxH_2 system. [d] The Cr(VI)−oxH_2 system.

Scheme 2. Possible Mechanism for the Formation of Cr(VI) and Cr(V)−Cr(VI) Oxalato Complexes in the Cr(VI)−oxH_2 System

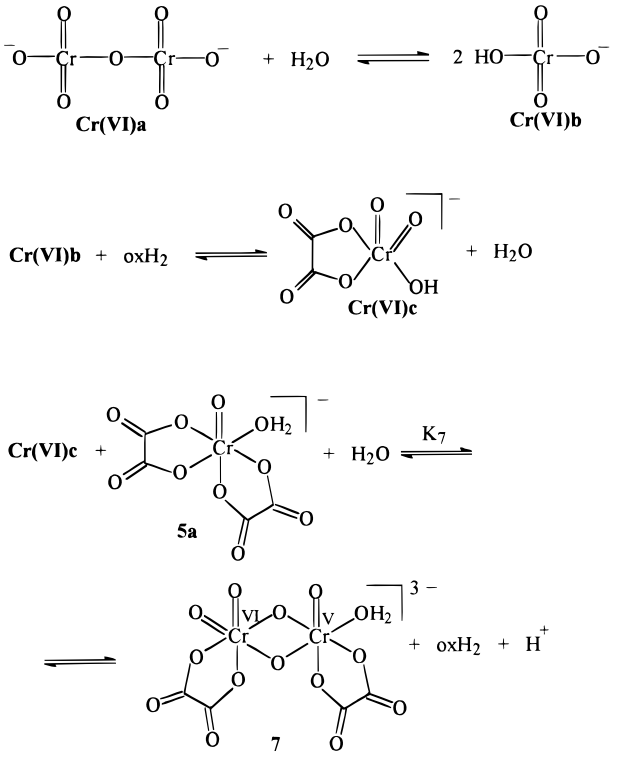

(eqs 6−8; Figures 2−4); (iii) comparison with well-characterized isoelectronic and isostructural V(IV) and V(V) oxalato complexes;[24−27] and (iv) empirical correlations between the known structures of Cr(V) complexes and their EPR parameters.[3] Together they provide unequivocal evidence for the structures of Cr(V) complexes corresponding to the observed EPR signals, as outlined below.

The g_{iso} and A_{iso} values of species **1** (Table 1) correspond[3] to those of Na[$Cr^{V}O$(ehba)$_2$] (a five-coordinate oxo complex with a distorted trigonal bipyramidal structure,[23] **1a** in Scheme 1). However, the statistically significant first term in eq 3 indicates that measurable amounts of monoligated complex **1b** (Scheme 1, Table S1) exist in equilibrium with **1a** under the studied conditions. Other evidence for the existence of an equilibrium between **1a** and **1b** in aqueous solutions was discussed previously.[2] Equations 3 and 4 show that signals **2** and **3** result from the stepwise replacement of ehba ligands by oxalate in **1a**. The

(23) Judd, R. J.; Hambley, T. W.; Lay, P. A. *J. Chem. Soc., Dalton Trans.* **1989**, 2205−2210.
(24) Form, G. E.; Raper, E. S.; Oughtred, R. E.; Shearer, H. M. M. *J. Chem. Soc., Chem. Commun.* **1972**, 945−946.
(25) Farrell, R. P.; Lay, P. A. *Appl. Magn. Reson.* **1996**, *11*, 509−519.
(26) Scheidt, W. R.; Tsai, C.; Hoard, J. L. *J. Am. Chem. Soc.* **1971**, *93*, 3867−3870.
(27) Farrell, R. P.; Lay, P. A. *Aust. J. Chem.* **1995**, *48*, 763−770 and references therein.

g_{iso} and A_{iso} values of **2** and **3**, which are close to those of **1**, suggest similar structures for these species (Scheme 1).[3] However, the significant decrease in the g_{iso} and increase in the A_{iso} values for the species **4**−**7** (Table 1) point to six-coordinate, octahedral structures for these Cr(V) complexes.[3] These assignments are confirmed by the dependences on ligand concentrations (eqs 6−8). The cis structure of **5a** and of the related complexes **4a**,**b** was suggested from the crystallographic data for the *cis*-$[V^{IV}O(OH_2)(ox)_2]^{2-}$ (isoelectronic with **5a**) and *cis*-$[V^{V}(O)_2(ox)_2]^{3-}$ complexes,[24,26] although the presence of some trans species is not precluded by the results. The complex expression for the ratio [**4**]/[**3**] (eq 6) can be explained by the formation of two species with similar g_{iso} values, **4a** and **4b** (Table 1, Scheme 1). The shifts to higher g_{iso} values for species **4a**,**b** in comparison with **5a** are consistent with the fact that OH^- and oxH^- are stronger electron donors than the H_2O ligand.[3] The decay of the EPR signal due to **4** at prolonged reaction times, or in the presence of added Cr(III) (Figure 2), are consistent with a decrease in the $[oxH_2]$ due to the formation of CO_2 and Cr(III) oxalato complexes. The decrease in the intensity of the EPR signal due to **4** with an increase in the $[Cr(VI)]_0$ (Figure 4a,c; Table S2) is explained by the decrease in the $[oxH_2]$ due to the formation of Cr(VI) oxalato complexes (Scheme 2).

The formation of a Cr(V) monooxalato complex **5b** (Scheme 1) was previously suggested[3,11] to explain the formation of a "shoulder" **6** in EPR spectra of the Cr(VI)−oxH_2 system (Figures 2−4). However, the results of the more detailed studies described here, including variations in $[H_2O]$ and the experiments at high $[Cr(VI)]_0$ and low $[oxH_2]_0$ (Table S2), are not consistent with the formation of significant amounts of Cr(V) monooxalato complexes in the Cr(VI)−oxH_2 system. Furthermore, the formation of species **6** (although in smaller amounts) was also observed in the Cr(V)−$ehbaH_2$−oxH_2 system. The presence of **6** in the latter system is especially evident at low acidities (Figure 1c). Under these conditions, taking into account the presence of excess $ehbaH_2$ (which is a much stronger ligand for Cr(V), than oxH_2), the formation of Cr(V) monooxalato complexes is unlikely. Therefore, an alternative explanation for the nature of species **6** was proposed (see below). However, a presence of small amounts of **5b**, which cannot be distinguished from **5a** due to the similar g_{iso} values,[28] is not excluded for the Cr(VI)−oxH_2 system, and such species are likely to be more important at lower concentrations of oxH_2 than were used here. However, the system is more difficult to quantify at lower $[oxH_2]/[Cr(VI)]$ ratios.

A clue to the nature of species **6** was the time dependence of the EPR spectra for the Cr(VI)−oxH_2 system (Figure 2a,b; Table S2). The growth of the relative signal intensity of **6** with time suggests its connection with an increase in the [Cr(III)] during the reduction of Cr(VI). The experiments in the presence of added Cr(III) (Figure 2c) confirmed this assumption. However, signal **6** cannot be due to a Cr(III) center, as the latter gives much broader EPR signals, which are difficult to observe at room temperature in aqueous media. Therefore, the formation of mixed-valence Cr(III)−Cr(V) species is assumed. Signal **6** is thought to be due to an oxalato-bridged species.[29] Quantitative data on [Cr(V)] and [Cr(III)] changes with time are required for more detailed studies of the possible structures of the Cr(III)−Cr(V) oxalato complexes, formed during the Cr(VI) + oxH_2 reaction. The relative broadness of the EPR signal due to **6** can be explained by the influence of paramagnetic Cr(III) ion on the signal of Cr(V), as well as by the presence of several overlapped signals due to the different Cr(III)−Cr(V) oxalato complexes.[29] The shift to lower g_{iso} values for **6** in comparison with **5** is probably due to the electron acceptor nature of the Cr(III) substituent, making it a weaker bidentate oxygen donor.[3] The formation of mixed-valence Cr(V)−Cr(III) complexes with macrocyclic ligands during the photolysis of the corresponding Cr(III) complexes has been reported.[30]

The natures of the species giving rise to signal **7** (mixed-valence Cr(V)−Cr(VI) complexes) are evident from (i) the linear growth of signal **7** with increasing $[Cr(VI)]_0$ (Figure 4a,c; eq 8); (ii) the relative decay of signal **7** during the course of the Cr(VI) + oxH_2 reaction (Figure 2a,b); (iii) the absence of the signal due to **7** in the Cr(V)−$ehbaH_2$−oxH_2 system (Figure 1); and (iv) the shift to lower g_{iso} values in comparison with the other EPR signals (Table 1), suggesting the presence of a weak electron donor ligand.[3] The relative broadness of signal **7** is consistent with the larger size of dimeric Cr(V)−Cr(VI) species in comparison with the monomeric Cr(V) complexes and/or the presence of several species. The lower g_{iso} value of the Cr(V)−Cr(VI) dimer compared to the Cr(III)−Cr(V) complex is also consistent with the greater electron-withdrawing effect of Cr(VI) in comparison with Cr(III). To our knowledge, no mixed-valence Cr(V)−Cr(VI) complexes have been described previously. The assignment of the structure and formation mechanism for species **7** requires a knowledge of the structures of Cr(VI) complexes in acidic aqueous solutions of oxH_2. The NMR spectroscopic studies[31] with the use of ^{13}C-labeled oxH_2 (in aqueous acetic acid solutions under similar pH and $[oxH_2]$ conditions) provided evidence for the existence of Cr(VI) mainly as a monooxalato complex (**Cr(VI)c** in Scheme 2).[31] The results of quantitative processing of EPR spectra are consistent with the assumption that practically all of Cr(VI) exists in the form of a monooxalato complex at $[oxH_2]_0 \geq 5[Cr(VI)]_0$ ($X = 1.0$ in eq 2). Furthermore, the results of experiments with $[oxH_2]_0 < 5[Cr(VI)]_0$, when Cr(VI) is partially complexed with oxalate ($X = 0.13-0.95$, see Table S2), suggest that only a Cr(VI) monooxalato complex participates in the formation of **7** (as the multiplier X is present in eq 8). The above-mentioned facts, together with the form of eq 8, allowed us to propose structure **7** (Scheme 2) for the main mixed-valence Cr(V)−Cr(VI) oxalato complex in aqueous media.[32] The shift in the EPR signals due to **7** to even lower g_{iso} values in water−sulfolane mixtures

(28) The similarity of the g_{iso} values for the complexes **5a** and **5b** is predicted by the known dependences between donor−acceptor properties of the ligands and g_{iso} values of Cr(V) complexes.[3]

(29) The formation of Cr(V) adducts with different forms of Cr(III) present in the reaction mixture (for example, **Cr(III)a**−**c** in Scheme 2) is expected. These adducts can include both oxalato- and oxo-bridged Cr(III)−Cr(V) complexes. However, most of these mixed-valence complexes will not result in such sharp EPR signals at room temperature due to interactions of the paramagnetic Cr(III) and Cr(V) centers. It is unclear as to the nature of the species giving rise to signal **6**, but the most likely species would be Cr(III)−Cr(III)−oxalato−Cr(V) trimers. Rapidly relaxing Cr(III) dimers with hydroxo and other bridges are common in the aqueous chemistry of Cr(III), and such dimeric centers bound to Cr(V) via an oxalato bridge would minimize broadening of the Cr(V) signal. Such a species appears to be the most viable structure to account for signal **6**.

(30) Niemann, A.; Bossek, U.; Haselhorst, G.; Wieghardt, K.; Nuber, B. *Inorg. Chem.* **1996**, *35*, 906−915.

(31) Farrell, R. P.; Maxwell, I. A.; Lay, P. A. To be submitted for publication.

(32) The presence of two μ-O atoms in the structure of the Cr(V)−Cr(VI) dimer, **7**, is consistent with the structure of the crystallographically characterized Cr(V)−Cr(V) dimer, di-μ-oxobis[oxo(perfluoropinacolato)chromate(V)] (Nishino, H.; Kochi, J. K. *Inorg. Chim. Acta*, **1990**, *174*, 93−102). However, alternative structures of the complex **7**, including oxalate as a bridging ligand, cannot be ruled out.

(Figure 4a,b) points to the possible formation of Cr(VI)−Cr(V)−Cr(VI) oligomers under these conditions.

Data obtained from EPR spectroscopy at room temperature cannot exclude the formation of Cr(V) dimers, which would be EPR-silent under these conditions.[2] However, the low-temperature EPR experiments[11] for the Cr(VI)−oxH_2 system did not reveal any signals with $g \sim 4$, which would correspond to such dimers.

Thus, both five-coordinate (**3**) and six-coordinate (**4**−**7**) Cr(V) oxalato complexes are formed in comparable amounts during the reduction of Cr(VI) by oxH_2 in acidic aqueous solutions. By contrast, in the case of isoelectronic V(IV) oxalato complexes, the six-coordinate form is dominant (and has been crystallized),[24] although the presence of small amounts of a five-coordinate form in solutions has been shown by EPR spectroscopy.[25] This difference in preference for six- over five-coordinate species is consistent with the smaller radius of the Cr(V) ion in comparison with V(IV).

Implications for the Mechanisms of Cr(VI) Reduction by oxH_2 in Acidic Aqueous Solutions. The obtained detailed knowledge on the structures of Cr(V) and Cr(VI) oxalato complexes allowed us to reassign the mechanism[7,8] of the Cr(VI) + oxH_2 reaction in acidic aqueous solutions. The results (Table 2, Figure S5) unequivocally establish that Cr(V) exists mainly in the form of bis-oxalates **3** and **5a** (Scheme 1) under the studied range of pH values and [oxH_2]. This is inconsistent with the earlier suggestions of Srinivasan and Roček[8] about the dominance of monooxalato Cr(V) complexes. The formation of the tris-oxalato/oxo species **4a** has been shown experimentally, and the possible presence of small amounts of monooxalato species **5b** has been assumed (Scheme 1). The structures of these Cr(V) complexes make them suitable for intramolecular two-electron reductions via a hydride transfer mechanism (Scheme 3). The mechanism of Cr(V) reduction to Cr(III), proposed by Scheme 3, explains the following experimental observations: (i) a higher reactivity of Cr(V), in comparison with Cr(VI), in the reaction with oxH_2; (ii) the formation of Cr(III)−Cr(V) and Cr(V)−Cr(VI) adducts and the absence of evidence for the formation of Cr(V)−Cr(V) dimers in the Cr(VI)−oxH_2 system, as the high reactivity of Cr(V) makes its concentration much lower than those of Cr(VI) and Cr(III); and (iii) the formation of mixtures of Cr(III) aqua complexes and mono- and bis-oxalato complexes[7] as the products of Cr(VI) reduction by oxH_2 (however, this may also be due partially to the slow ligand exchange reactions of the Cr(III) complexes, in parallel with the redox reactions).

The present work is consistent with the results of recent ^{13}C NMR spectroscopic studies,[31] showing the existence of Cr(VI) mainly in the form of a monooxalato complex in aqueous solutions in the presence of excess oxH_2. By contrast, the earlier kinetic studies[7,8] assumed that $[HCrO_4]^-$ is the main form of Cr(VI) under these conditions, with Cr(VI) mono- and bis-oxalato complexes being present as minor intermediates. Finally, the formation and properties of Cr(IV) bis-oxalato complex have been described recently.[33] Thus, the new data on the structures and properties of Cr(VI/V/IV) oxalato complexes allowed us to reassign the mechanism of the Cr(VI) reduction by oxH_2 in acidic aqueous solutions. The most likely sequence of reactions leading to the Cr(V) complex **5b** is given in Scheme 4. The subsequent rapid equilibria leading to the different forms of Cr(V) are presented in Schemes 1 and 2. Finally, Scheme 3 shows the possible mechanisms for the formation of Cr(III) products. As the formation of Cr(V) is much slower than its further reduction (as it was concluded from the comparison of the reaction rates in the Cr(V)−ehbaH_2−oxH_2 and Cr(VI)−oxH_2 systems), the overall reaction rate can be presented by eq 9 (see Scheme 4):

$$-\mathrm{d[Cr(VI)]}/\mathrm{d}t = \mathrm{d[Cr(IV)]}/\mathrm{d}t = k_2[\mathbf{Cr(VI)d}][oxH_2] \quad (9)$$

Assuming that, in the presence of a large excess of oxH_2 (pseudo-first-order conditions), **Cr(VI)c** is the main form of Cr(VI), but **Cr(VI)d** (Scheme 4) is the steady-state intermediate,[34]

Scheme 3. Possible Mechanism for the Formation of Cr(III) Oxalato Complexes in the Cr(VI)−oxH_2 System

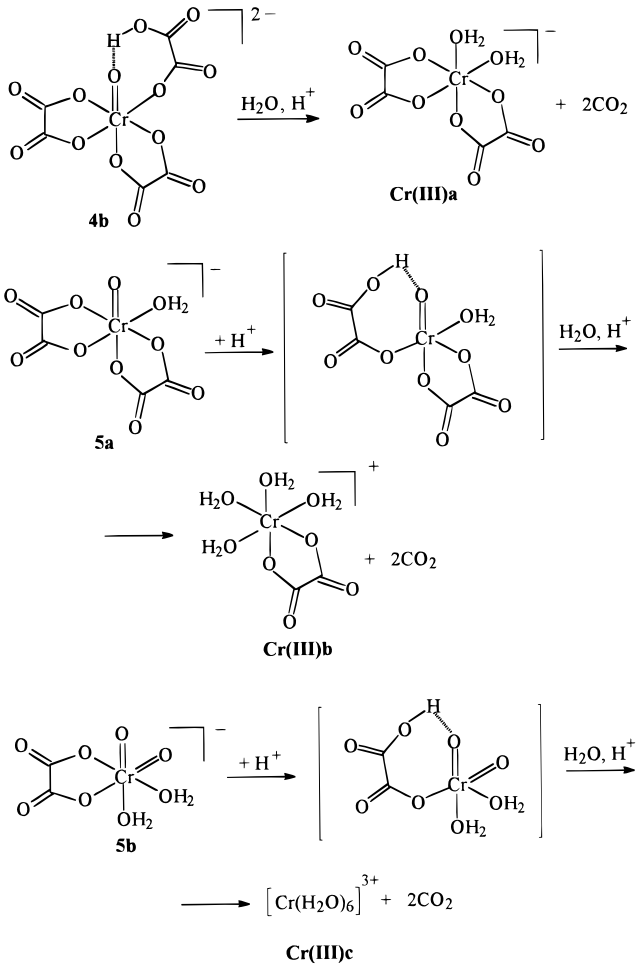

(33) The Cr(IV) bis-oxalato complex (its proposed structure is shown in Scheme 4) has been generated *in situ* by ligand exchange reactions of Cr(IV)−ehba complexes with oxalate. The Cr(IV)−ox complex is relatively stable at pH = 4−5 ($\tau_{1/2} \sim 90$ min at $[Cr(IV)]_0 = 0.1$ mM and 25 °C) and rapidly decomposes in acidic media ($\tau_{1/2} \sim 10$ s at pH = 1) (Codd, R.; Lay, P. A.; Levina, A. *Inorg. Chem.* **1997**, *36*, 5440−5448). The decomposition of Cr(IV)−ox in acidic solutions (pH = 0−1.5) leads entirely to Cr(III) (not Cr(V) or Cr(VI)). The decomposition rate increases sharply with increasing [H^+] and is practically independent of $[oxH_2]_0$ and $[Cr(VI)]_0$ (Levina, A. Unpublished results).

(34) The bis-oxalato complexes, *cis*-$[V^VO_2(ox)_2]^{3-}$ and *cis*-$[V^VO(OH)(ox)_2]^{2-}$, are the main V(V) species observed by NMR techniques in acidic aqueous solutions in the presence of excess oxH_2.[11,27] In the isoelectronic Cr(VI)−oxH_2 system, the formation of bis-oxalato complexes is also expected to be thermodynamically favorable. However, the experimental evidence (refs 11 and 31 and the current work) points to Cr(VI) existing mainly in the monooxalato form. This suggests that the Cr(VI) bis-oxalato intermediates are rapidly consumed in the following redox reactions. Therefore, the steady-state approximation for the complex **Cr(VI)d** (Scheme 4) is appropriate.

Scheme 4. Possible Mechanism for the Formation of Cr(V) Species during the Cr(VI) Oxidation of oxH_2

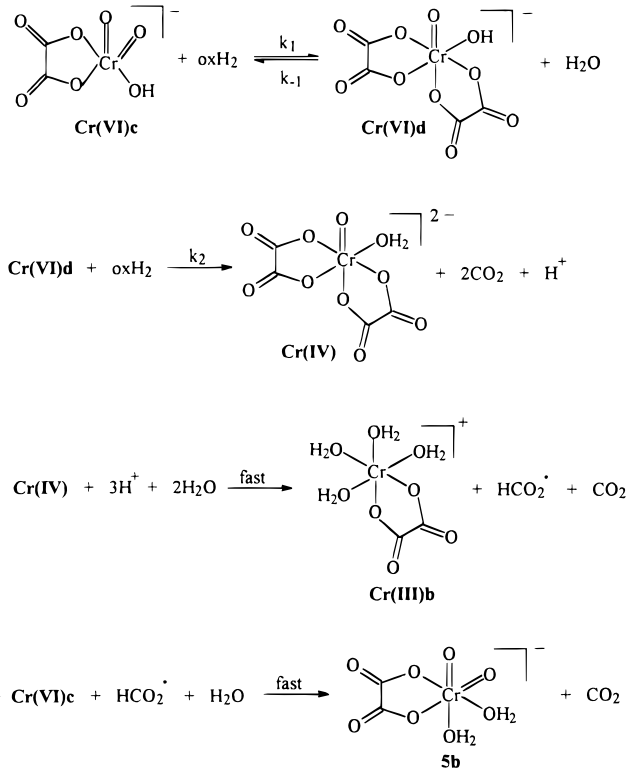

the following expression for the pseudo-first-order rate constant (eq 10) can be derived:

$$k_{obs} = k_1 k_2 [oxH_2]^2/(k_{-1} + k_2[oxH_2]),\ s^{-1} \qquad (10)$$

where $[oxH_2]$ is the concentration of undissociated oxH_2.

The following experimentally observed[7] kinetic features of the Cr(VI) + oxH_2 reaction ($[H^+] = 0.010-1.0$ M; 25 °C) are predicted by eq 10: (i) the reaction order with respect to oxH_2 changes from second to first with an increase of $[oxH_2]$; and (ii) the reaction rate is practically independent of $[H^+]$, apart from the influence of acidity on $[oxH_2]$. The published kinetic data[7] are well described by eq 10 (Figure 5),[35] thus supporting the validity of the proposed mechanism (Scheme 4). The proposed mechanism for the decomposition of the Cr(IV) oxalato complex (Scheme 4) is consistent with the known properties of this complex,[33] as well as with the observed formation of radical species (presumably $HCO_2^{\bullet}$) in the reaction media.[7] According to Scheme 4, equivalent amounts of Cr(III) and Cr(V) are formed practically simultaneously during the Cr(VI) + oxH_2 reaction. This explains the appearance of EPR signal **6**, corresponding to the Cr(III)−Cr(V) mixed-valence species, even in the early stages of the redox reaction. The alternative route leading to Cr(V), namely, the Cr(VI) + Cr(IV) reaction, is unlikely because the Cr(VI) reaction with the Cr(IV) oxalato complex at pH = 0−1.5 has been shown to be much slower than the acid-catalyzed decomposition of the Cr(IV) complex.[33]

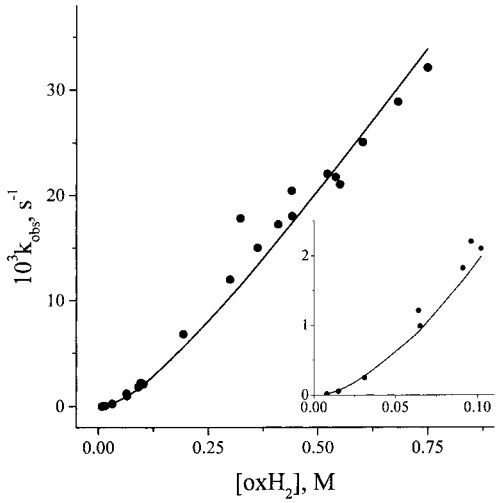

Figure 5. Application of eq 10 ($k_1 = (6 \pm 1) \times 10^{-2}$ M^{-1} s^{-1}; $k_2/k_{-1} = 5 \pm 1$ M^{-1}) to the published kinetic data[7] for the Cr(VI) + oxH_2 reaction in acidic aqueous solutions, 25 °C. Points are the experimental data, and the solid line is calculated from eq 10.

Acknowledgment. The financial support of this project from an Australian Research Council (ARC) grant (to P.A.L.) and an ARC infrastructure grant for the EPR instrumentation are gratefully acknowledged.

Supporting Information Available: Typical examples of experimental and simulated EPR spectra, simulation results for EPR spectra of the Cr(V)−ehbaH_2−oxH_2 and Cr(VI)−oxH_2 systems, and relations between experimental and estimated concentration ratios for separate species (17 pages). Ordering information is given on any current masthead page.

IC971070I

(35) The large scatter of the experimental data (Figure 5) is probably because of the large errors in determination of $[oxH_2]$ (the deprotonation equilibria for oxH_2 were estimated[7] on the basis of amounts of $HClO_4$ added into the system, and the increase of $[H^+]$ due to deprotonation of oxH_2 was not taken into account).